

## Autonomous Surgical Robotics Using 3-D Ultrasound Guidance: Feasibility Study

JOHN WHITMAN, MATTHEW P. FRONHEISER, NIKOLAS M. IVANCEVICH  
AND STEPHEN W. SMITH

*Department of Biomedical Engineering  
Duke University  
Durham, NC 27708  
ssmith@duke.edu*

The goal of this study was to test the feasibility of using a real-time 3D (RT3D) ultrasound scanner with a transthoracic matrix array transducer probe to guide an autonomous surgical robot. Employing a fiducial alignment mark on the transducer to orient the robot's frame of reference and using simple thresholding algorithms to segment the 3D images, we tested the accuracy of using the scanner to automatically direct a robot arm that touched two needle tips together within a water tank. RMS measurement error was 3.8% or 1.58 mm for an average path length of 41 mm. Using these same techniques, the autonomous robot also performed simulated needle biopsies of a cyst-like lesion in a tissue phantom. This feasibility study shows the potential for 3D ultrasound guidance of an autonomous surgical robot for simple interventional tasks, including lesion biopsy and foreign body removal.

Key words: Autonomous; biopsy; robotics; segmentation; 3D ultrasound.

### INTRODUCTION

We have previously investigated the feasibility of using real time 3D laparoscopic ultrasound to guide a surgical robot.<sup>1</sup> In that study, a 1-cm diameter probe for RT3D<sup>2</sup> was used laparoscopically for *in vivo* imaging of a canine. The probe was operated at 5 MHz and used to image the spleen, liver and gall bladder as well as to guide hand-held surgical instruments. Furthermore, the three-dimensional (3-D) measurement system of the volumetric scanner, used with this probe was tested as an automatic guidance mechanism for a robotic linear motion system in order to simulate RT3D/robotic surgery integration. Using the scanner measurement software with the B-mode and C-mode images displayed from the real time 3D scan, the remote operator measured spatial coordinates that were used to direct a robotically-controlled needle toward desired *in vitro* targets as well as targets in a postmortem canine. The root mean squared (RMS) error for these measurements was 1.34 mm using a fiducial alignment mark on the transducer housing and 0.76 mm using only the measurement software of the 3D scanner to compute a path between two targets in the volumetric scan. In similar fashion, 2D ultrasound scanners have been used for image guided surgical robotics.<sup>3,4</sup> More recently, we demonstrated analogous results<sup>5</sup> using 3D catheter transducers with the 3D measurement software of the real-time scanner to direct a robot arm that touched two needle tips together within a water tank and inside a vascular graft. RMS measurement error ranged from 2.4 - 3.4 mm for two catheter designs.

The goal of this paper is to extend our previous results of 3D ultrasound guidance to guide an autonomous robot in simulated interventional procedures by using real-time 3D ultrasound imaging and a commercial transthoracic matrix array combined with simple image segmentation analysis.

## METHODS

Real-time, 3-D ultrasound was developed at Duke University by Smith et al<sup>6</sup> and von Ramm et al<sup>7</sup> for cardiac imaging and commercialized by Volumetrics Medical Imaging. The Duke/VMI scanner (Volumetrics Medical Imaging, Durham, NC) produces a 65°- 90° pyramidal scan at rates up to 30 volumes per second. The scanner simultaneously displays two B-scans and up to three parallel C-scans at any angle and depth as well as real time 3D volume rendering, 3-D color and 3-D pulsed Doppler. Each 3D ultrasound scan is comprised of  $64 \times 64 = 4096$  B-mode lines, including 512 samples per image line yielding 2 MB of data per 3D scan. Echo amplitude is eight bits ranging from 0 to 255. For this study, we used the commercial VMI transthoracic matrix array, which includes 440 transmit channels and 256 receive channels operating at 2.5 MHz as previously described.<sup>8</sup>

The robot used for these feasibility experiments was a Gantry III Cartesian Robot Linear Motion System manufactured by Techno-Isel (Techno, Inc., New Hyde Park, NY) using a Model H26T55-MAC200SD automated controller that accepts input commands and 3-D coordinates from a connected computer. The XY stage (model HL32SBM201201505) is a stepper motor design providing 340 mm  $\times$  290 mm of travel on a 600 mm  $\times$  500 mm stage. The Z-axis slide (model HL31SBM23051005) provides 125 mm of vertical clearance and allows 80 mm of travel in the z-dimension.

Figure 1 shows a simple schematic of the 3-axis robot holding a probe needle and the 3D scanner imaging a vertical target needle in a water tank. Etched into the side of the 3-D matrix array transducer was a fiducial crosshair whose coordinates were input to the robot controller. Thus the robot's frame of reference was zeroed on the transducer's fiducial spot.

In the current study, at a user-controlled trigger, the scanner halted and the latest volume of 3D ultrasound data was automatically transferred over a Category 5 Ethernet connection via Universal Data Protocol to a PC controller which was running our Matlab (Mathworks, Natick, MA) image analysis software. No further user input was required. Data transmission and loading of the 2 MB file into the Matlab program required approximately 15 seconds. Note that the complete 3D scan data was transferred with no user selection of the target or choice of image slices. Also note that the image data was not scan converted but was transmitted in  $r, \theta$  coordinates including depth,  $r$ , azimuth angle,  $\theta$ , and elevation angle,  $\phi$ , as previously described.<sup>6</sup>

Figure 2a illustrates an example volume rendered view of a 3D scan of a target needle (1 mm in diameter and 30 mm long) in a water tank whose echo data was transmitted to the robot controller for the task of needle tip touching. The 3D rendered image shows the tip of the target needle (solid arrow) with a tail of reverberation echoes within the needle. Also shown in the 3D image is an echo cluster artifact resulting from other reverberations within the water tank (dotted arrow). To segment the image and isolate the target needle tip, our Matlab script automatically rejected all echoes below a preset threshold and calculated the 3D location of all remaining echoes. Figure 2b shows three orthogonal views of the segmented image of the needle tip in figure 2a when the threshold setting is above a level of 200. Figure 2c shows the location of the needle tip (black dot) superimposed on the pyramidal scan icon by the Matlab program. These images were automatically displayed to the passive observer

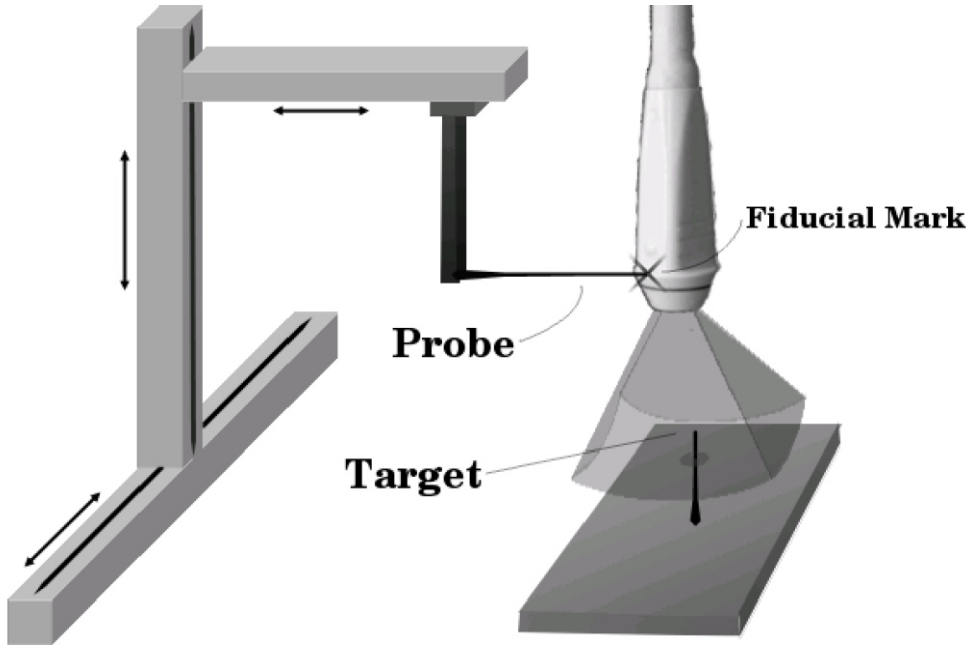


**FIG. 1** Schematic of the autonomous robot experiment. The horizontal probe needle was attached to the robotic arm while the vertical target needle was fixed within a piece of rubber.



**FIG. 2** Volume rendered 3D image of needle (a), simultaneous cross sections after image thresholding (b) and needle tip location in pyramidal icon (c).

during the image segmentation process. Figure 2c also shows a circular region of exclusion at the apex of the pyramid, which the probe needle could not enter, to prevent collisions between the probe needle and the transducer. The complete image segmentation process required approximately one second.

The location of the target needle tip in the coordinate system of the scanner was then converted into the coordinate system of the robot as previously described,<sup>1</sup> and the distance between the target tip and probe tip was calculated by simply subtracting the coordinates of the probe needle tip resting at the fiducial mark from those of the target needle tip. The robot then moved its arm holding the probe needle the corresponding distances in each rectangular coordinate. Since the robot was capable of only 3-axis motion it was important to align all mechanical components with vertical and horizontal axes. The robot movements required approximately five seconds.

After the robot arm had completed movement, the error in each coordinate was measured by recording the distance needed to manually jog the robotic arm until the probe needle tip

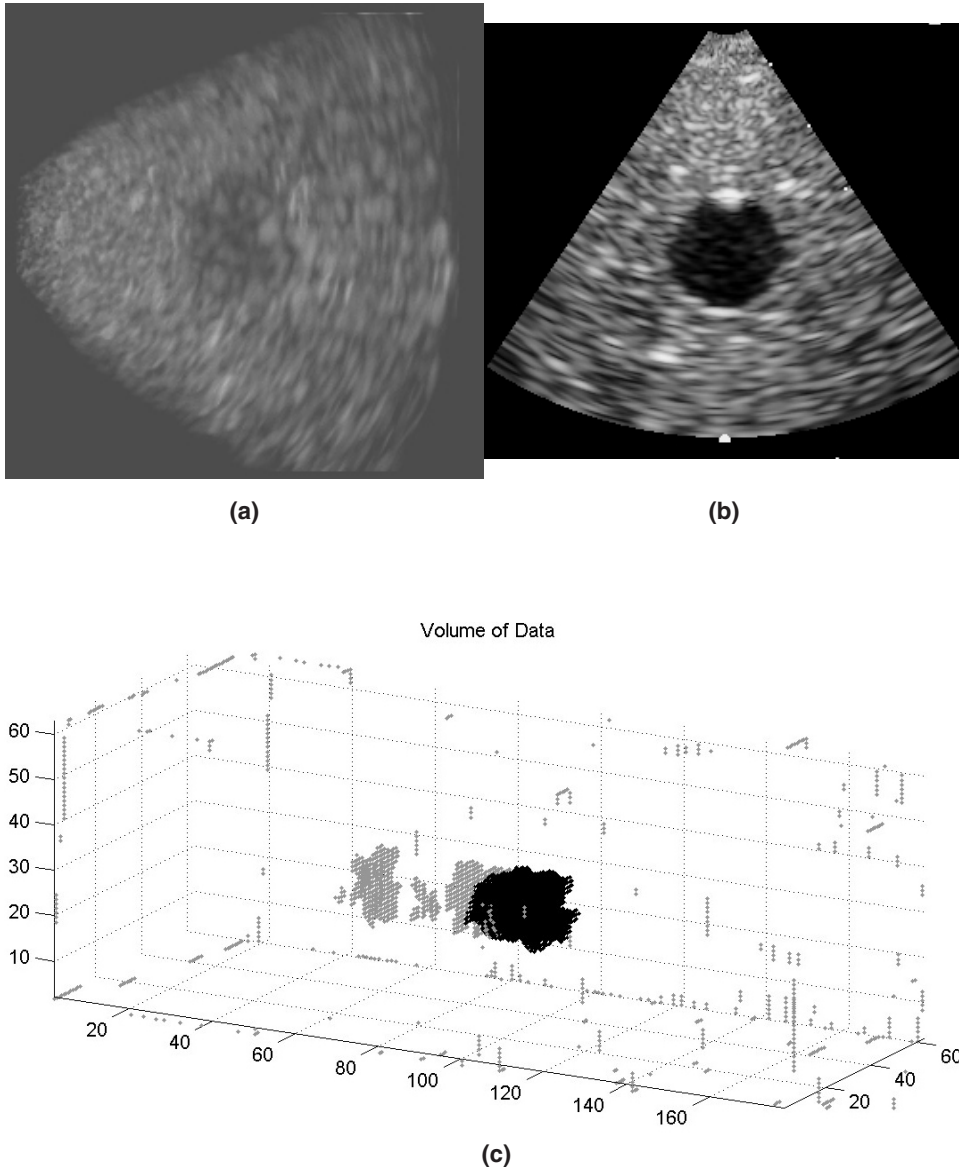


**FIG. 3** Volume rendered 3D image of cyst in tissue mimicking phantom (a), simultaneous cross section (b), distribution of 3D image voxels after median filtering and thresholding (c).

touched the tip of the target needle based on visual inspection. RMS error was then calculated. Needle tips were originally separated by several cm, and the procedure was repeated 5 times.

A second experimental study of 3D ultrasound guidance of an autonomous robot was performed to simulate the task of a cyst biopsy. We suspended a roughly spherical anechoic lesion approximately 2 cm in diameter (a water filled balloon) in a tissue-mimicking phantom developed by Madsen et al<sup>9</sup> consisting of a slurry of agar spheres containing graphite scatterers. As in the needle tip experiment above, the Volumetrics system acquired a 3D scan of the object and transmitted the complete 3D volume of echo data to the robot controller with no slice selection or target selection by a human observer. Figure 3a shows a real-time volume

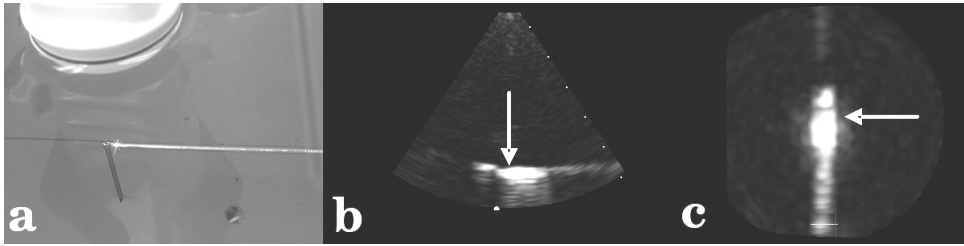


**FIG. 4** Photograph of needle touch experiment (a), simultaneous B-scan (b) and C-scan (c) of needle touch experiment.

rendered image of the lesion immersed in the tissue-mimicking slurry. Note the overlying tissue which obscures the lesion. Figure 3b shows a single B-mode slice of the lesion for illustration purposes only. Note the presence of bright inhomogeneities in the tissue mimicking material.

For this task, we modified the image segmentation software. The Matlab scrip first applied a  $3 \times 3 \times 3$  median filter to the pixels of the 3D scan to smooth the image speckle. Next, all voxels were rejected whose amplitude fell above a selectable threshold value of one quarter of the mean echo amplitude of the volume. The resulting map of the remaining voxels is shown in figure 3c wherein the cyst voxels (black) stand out as the largest group. Other remaining voxels correspond to minima in the speckle background. Finally, the software located the median voxel in three space of the largest group of contiguous voxels that approximated the center of the cyst. These software operations required approximately five seconds. As described above, these coordinates were then passed to the robot that directed the probe needle to the center of the lesion. No visual error measurements were made in this experiment due to the optical opacity of the phantom. The experiment was repeated five times.

## RESULTS

Figure 4 illustrates the results of one typical needle touch experiment including a photograph (Fig. 4a) showing the face of the matrix array transducer and the horizontal probe needle tip in close proximity to the vertical target needle tip. In like manner, figure 4 shows a B-mode image plane (Fig. 4b) and simultaneous C-mode image plane (Fig. 4c) from the 3D scanner that was used to monitor the autonomous robot operation. The figures show simultaneous perpendicular long axis views of the probe needle (solid arrow) as its tip is about to make contact with the target needle tip. For a set of five independent experiments wherein the target needle was repositioned requiring an average robot motion of 41.2 mm, a maximum error of 2.00 mm and an average RMS error 1.58 mm or 3.82 %.

Figure 5 shows analogous data for one typical trial of the task of the simulated cyst biopsy performed by the autonomous robot while monitored by the 3D scanner as the needle tip contacts the cyst surface. Figure 5 includes a long axis view of the probe needle in a B-mode mode plane (Fig. 5a). Note that the needle tip is accurately aligned in depth with the center of the lesion. Note also the reverberation tail from the probe needle. Figure 5b shows the simultaneous orthogonal long axis view in a C-scan of the probe needle tip at the surface of the cyst. Note that this view of the needle tip shows slight lateral misalignment with the center of the cyst. In like manner, figure 5c shows a simultaneous B-mode short axis view of the needle tip accurately aligned in depth but slightly off-center laterally.

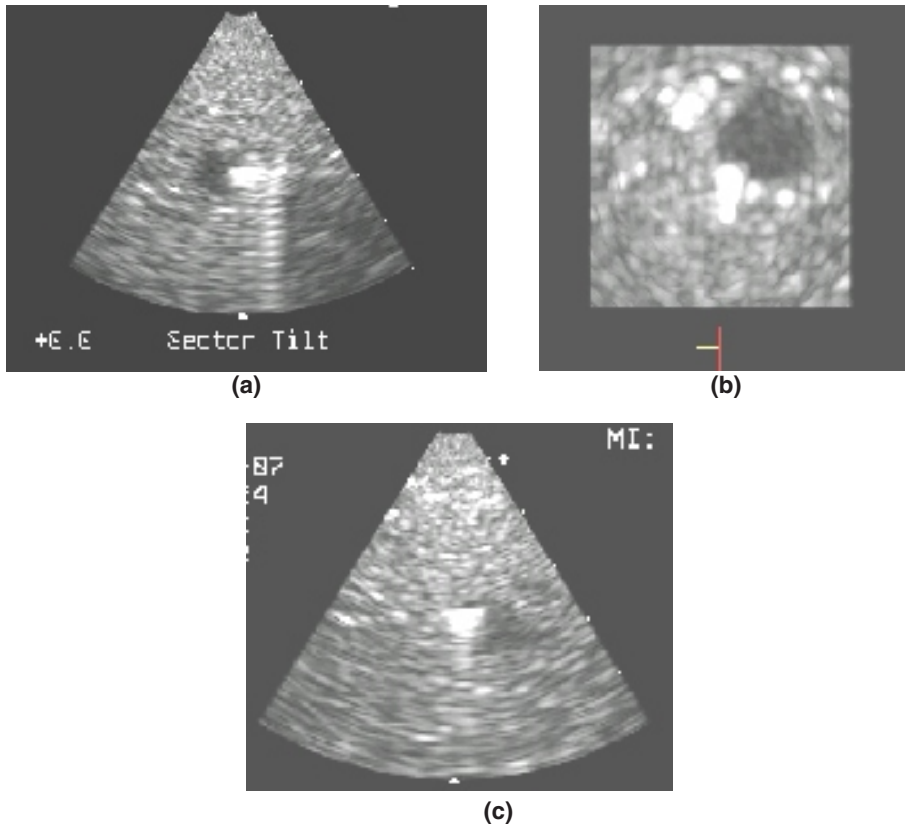


**Fig. 5** Simultaneous orthogonal views from 3D ultrasound scan of simulated needle biopsy of cyst including: (a) long axis B-scan, (b) long axis C-scan and (c) short axis B-scan.

## DISCUSSION

We have demonstrated feasibility of autonomous robot operation to accomplish simulated surgical tasks under the guidance of 3D ultrasound imaging combined with image segmentation. The RMS error for the task of needle tip touching was 1.58 mm, which compared favorably to our previously-published results of 1.34 mm for a human observer using the 3D scanner's measurement software to accomplish a similar task. The small measured error is encouraging given the limitations of the experiment including: (1) the restrictions of only 3 axis motion by the robot, (2) the limited spatial resolution of the real time 3D scanner and (3) the simple image thresholding software used to segment the 3D ultrasound images.

For the more difficult task of a cyst biopsy, the error appeared larger due to the increased complexity of the target and the simple segmentation algorithm. However, in each trial, the needle squarely impacted the surface of the cyst to enable a biopsy.

Another issue for further investigation is the potential error in a robotic surgical intervention due to velocity inhomogeneities in tissue. For example, fat and muscle sound velocity can differ by as much as 10%, which would reduce the accuracy of location for any target such as a lesion or foreign body embedded in tissue. This topic has been long been of interest in our laboratory and others.<sup>10</sup> We note, however, that this problem is not exclusive to a surgical robot but arises for all interventional ultrasound biopsies that are performed many times daily by a human operator.

The most significant limitation of this feasibility study was the lengthy time required for 3D data transfer and loading into the Matlab image analysis program. However, more modern data transmission and faster software would reduce that time by at least an order of magnitude. In clinical use it would also be necessary to reduce significantly the five seconds required for the robot to move through its task. This problem could be solved through a state-of-the-art surgical robot, such as the DaVinci system (Intuitive Surgical, Sunnyvale, CA) with multiple arms that could exploit the advantages of real time 3D ultrasound and coordinate the motion of the 3D transducer with the control of the surgical tools. In addition, the well-known technologies of respiration gating and cardiac gating would ameliorate the problems associated with tissue motion during the surgical procedure. We also note that there are much more sophisticated image analysis technologies<sup>11</sup> that could be applied to more complex tasks for an autonomous surgical robot. Finally, the real time 3D color Doppler features of the volumetric scanner offer additional capabilities for autonomous robotic surgery in targeting or avoiding blood vessels.

## CONCLUSION

The goal of this study was to test the feasibility of using a real-time 3D (RT3D) ultrasound scanner with a matrix array transducer probe to guide an autonomous surgical robot. Employing a fiducial alignment mark on the transducer to orient the robot's frame of reference and using simple thresholding algorithms to segment the 3D images, we tested the accuracy of using the scanner to automatically direct a robot arm in simple simulated surgical tasks including needle tip touching and a simulated cyst biopsies. This feasibility study shows the potential for 3D ultrasound guidance of an autonomous surgical robot for simple interventional tasks including lesion biopsy and foreign body removal.

## REFERENCES

1. Pua EC, Fronheiser MP, Noble J, et al. 3-D ultrasound guidance of surgical robotics: a feasibility study. *IEEE Trans Ultrason Ferroelec Freq Contr* 53, 1999-2008 (2006).
2. Pua EC, Idriss F, Wolf PD, Smith SW. Real-time 3D transesophageal echocardiography. *Ultrasound Imaging* 26, 217-232 (2004).
3. Traumapod <http://www.sri.com/news/releases/03-28-05.html>.
4. Leven JBD, Kumar R, Zhang et al. DaVinci canvas: a telerobotic surgical system with integrated, robot-assisted, laparoscopic ultrasound capability, presented at Med Image Comput Comput Assist Interv Int Conf., 2005.
5. Whitman J, Fronheiser MP, Ivancevich NM, Smith SW. 3-D ultrasound guidance of surgical robotics using catheter transducers: feasibility study. *IEEE Trans Ultrason Ferroelec Freq Contr* (accepted) (2007).
6. Smith SW, Pavy HE, von Ramm OT. High speed ultrasound volumetric imaging system part I: transducer design and beam steering. *IEEE Trans Ultrason Ferroelec Freq Contr* 38, 100-108 (1991).
7. von Ramm OT, Smith SW, Pavy HE. High speed ultrasound volumetric imaging system part II: Parallel processing and display. *IEEE Trans Ultrason Ferroelec Freq Contr* 38, 109-115 (1991).
8. Light ED, Davidsen RE, Fiering JO, et al. Progress in two-dimensional arrays for real-time volumetric imaging. *Ultrasonic Imaging* 20, 1-15 (1998).
9. Madsen EL, Zagzebski JA, Insana MF, et al. Ultrasonically tissue-mimicking liver including the frequency-dependence of backscatter. *Med Phys* 9, 703-710 (1982).
10. Anderson ME, McKeag M, Trahey GE. The impact of sound speed errors on medical ultrasound imaging. *J Acoust Soc Amer* 107, 3540-3548 (2000).
11. Sonka M, Hlavac, V., Boyle, R. *Image Processing, Analysis, and Machine Vision* (PWS Publishing, Pacific Grove, CA, 1999).